

geofísica
internacional

Geofísica Internacional

ISSN: 0016-7169

silvia@geofisica.unam.mx

Universidad Nacional Autónoma de México
México

Tiscareño López, Mario; Báez González, Alma Delia; Izaurralde, César; Rosenberg, Norman J.;
Salinas García, Jaime

Modeling El Niño Southern Oscillation climate impact on Mexican agriculture

Geofísica Internacional, vol. 42, núm. 3, july-september, 2003, pp. 331-339

Universidad Nacional Autónoma de México

Distrito Federal, México

Available in: <http://www.redalyc.org/articulo.oa?id=56842305>

- How to cite
- Complete issue
- More information about this article
- Journal's homepage in redalyc.org

redalyc.org

Scientific Information System

Network of Scientific Journals from Latin America, the Caribbean, Spain and Portugal

Non-profit academic project, developed under the open access initiative

Modeling El Niño Southern Oscillation climate impact on Mexican agriculture

Mario Tiscareño López¹, César Izaurre², Norman J. Rosenberg², Alma Delia Báez González¹ and Jaime Salinas García³

¹ *Instituto Nacional de Investigaciones Forestales, Agrícolas y Pecuarias, Pabellón de Arteaga, Aguascalientes, México*

² *Battelle, Pacific National Northwest Laboratory, Washington, D.C., USA*

³ *Instituto Nacional de Investigaciones Forestales, Agrícolas y Pecuarias, Tamaulipas, México*

Received: September 3, 2000; accepted: April 15, 2001

RESUMEN

El fenómeno de El Niño Oscilación del Sur (ENOS) provoca anomalías climáticas en México con impactos significativos en la agricultura de temporal. Esta investigación simula el ENOS con el propósito de identificar anomalías climáticas durante los años El Niño y El Viejo (también conocido como años La Niña), y su consecuente desviación en los rendimientos de maíz y frijol. Los datos diarios procedentes de 275 estaciones meteorológicas distribuidas en el territorio Mexicano fueron usadas para distinguir el clima local durante los años de El Niño (EN), El Niño Extremo (ENE) y El Viejo (EV) respecto a los años de clima neutral, de acuerdo con el Índice the Anomalía Térmica de las aguas del océano Pacífico. El rendimiento de las cosechas fue estimado con un modelo de simulación del crecimiento vegetal bajo el modo de generación de clima para cada escenario ENOS. El esquema de modelaje aplicado por esta investigación permitió identificar las regiones de México que son sensibles a los eventos ENOS, y que por consiguiente sujetas a cambios en los rendimientos de los cultivos como resultado de las desviaciones de temperatura del aire y la precipitación durante la estación de crecimiento del cultivo en los años EN, SEN y EV.

PALABRAS CLAVE: ENOS, simulación, precipitación, temperatura, cultivos, erosión.

ABSTRACT

El Niño Southern Oscillation (ENSO) induces climate anomalies in Mexico that have significant impacts on rain-fed agriculture. This research simulates ENSO scenarios to identify climate anomalies during El Niño and El Viejo years (also known as La Niña years), and fluctuations in maize and bean crop yield. Daily weather data from 275 meteorological stations located throughout the country were used to distinguish local climate conditions under El Niño (EN), Strong El Niño (SEN), and El Viejo (EV) from those of Neutral years, based on the Thermal Anomaly Index of sea surface water of the Pacific ocean. Crop yields were assessed with a process-based crop growth model under weather generation using climate parameters of each ENSO scenario. The modeling scheme allowed the identification of regions of Mexico sensitive to ENSO events and susceptible to crop yield changes as a result of deviations in air temperature and precipitation occurring during the crop growing season in EN, SEN and EV years.

KEY WORDS: ENSO, simulation, crops, erosion, precipitation, temperature.

INTRODUCTION

El Niño Southern Oscillation (ENSO) is a term referring to sea surface water temperature increase in the tropical Pacific ocean associated with changes in wind direction due to barometric pressure oscillations in the Southern Pacific. ENSO events trigger climate anomalies in most of the American continent and other regions of the world. ENSO-related atmospheric and oceanic processes cause a decrease in plankton along the South American coast and a diminution of important marine species (Rasmusson, 1985; Glantz, 1996).

Meteorological information recorded since the beginning of the 20th century has enabled scientists to identify

the recurrence of dry and wet periods that coincide with periods of heating and cooling of sea surface waters of the Pacific ocean. More recently, a teleconnection between atmospheric and oceanic conditions in the region 4°S - 4°N, 150°W - 90°W of the tropical Pacific and the prevailing climate in various parts of the world was identified. Intensive meteorological and marine monitoring of the Pacific ocean allowed the description of El Niño events from the decades of the 80s and 90s, with a high degree of reliability (Trenberth and Brandstadter, 1992; Izaurre *et al.*, 1998).

The drought that affected a large extent of Mexico at the end of 1982 and during 1983, with damages near 600 million dollars, was caused mainly by El Niño 1982-83 (Canby, 1984). The national decline of maize production and

the abandonment of fields by farmers were triggered by the El Niño phenomenon. At least six of nine El Niño events that occurred after 1960 have caused significant slumps in maize production (Figure 1).

Studies on climate have been focused at exploring ENSO impact on agricultural productivity. Cane *et al.* (1994) identified crop yield reductions in rain-fed areas in Africa during warm phases of ENSO in the Pacific ocean. Financial analysts consider ENSO as an indicator for estimating crop prices, taking into account continental precipitation variations. This has raised expectations about the economic value of predictions of climate under the influence of ENSO as they are related to agricultural activities. Solow *et al.* (1997) estimate that recent improvements of climatic predictions in the United States of America have benefited US agriculture by more than 200 million dollars per year.

We present some results of modeling plant growth under ENSO, to estimate the impact of climate anomalies on the yield of crops cultivated under rain-fed conditions. The method is based on a probabilistic approach applied to biophysical processes simulated with a computer model calibrated with field data from different agricultural regions of Mexico. Changes in crop yield, resulting from hydrology and plant growth, were considered to assess the impact of ENSO on Mexican agriculture.

ENSO SCENARIOS

To model the ENSO phenomena, based on the concept of teleconnections, it was necessary to identify ENSO scenarios and to establish their relationship with the prevailing climate in different regions of the country. For this purpose, the Thermal Anomaly Index (τ) developed by the Japan Meteorological Agency was utilized, which is the sea surface water temperature (SST) of the 90°–150° W and 4°

N at 4° S geographical delimited region in the Pacific ocean. τ is the 5-month running mean of SST anomalies over the aforementioned region and an ENSO year covers the period from 1 October to 30 September. An El Niño (EN) year occurs when $0.5 \leq \tau < 2.0$ °C during six consecutive months, starting 1 October. An El Viejo (EV) year occurs when $\tau \leq -0.5$ °C. A year is Neutral (N) when $-0.5 < \tau < 0.5$ °C. A fourth category is Strong El Niño (SEN), assigned to those years when $\tau > 2.0$ °C for two consecutive months instead of six consecutive months for other scenarios. Considering a period with complete meteorological data from 1960 to 1989, six events have been classified as EN (1963, 1965, 1969, 1976, 1986 and 1987), two as SEN (1972 and 1982), seven as EV (1964, 1967, 1970, 1971, 1973, 1975 and 1988), and the rest as Neutral years.

Daily weather records from 1960 to 1989, obtained from 275 meteorological stations distributed throughout the country, were utilized to compute monthly climate parameters: mean and standard deviation of maximum and minimum air temperature, total and standard deviation of monthly precipitation, skewness coefficient of the precipitation normal distribution, transition probabilities for the occurrence of rain, and number of rainy days within the month.

THE EPIC MODEL

Climate and plant growth were simulated with the Erosion Productivity Impact Calculator (EPIC) model developed by Williams (1995). EPIC is a process-based continuous simulation model, which utilizes basic information of soils, climate and crop management to estimate crop yield and hydrologic responses like soil water erosion. Major components of the model are the stochastic weather generation, surface and subsurface hydrology, erosion sedimentation processes, nutrient cycling, plant growth, cultivation practices and accounts of the effects of pests and diseases on the simulated plant biomass. Governing equations of major simulated processes by EPIC are given in the Appendix.

The climate component of EPIC is a stochastic weather generator that applies a Markov chains scheme to produce series of daily precipitation (Nicks, 1974), and maximum and minimum air temperature correlated with solar radiation (Richardson, 1981). For the generation of synthetic series of EN, EV, SEN and N scenarios, the stochastic dependence of wet and dry days within the actual climate series obtained from each meteorological station was calculated. This made it possible to estimate the transition probabilities of rainy days and dry days for the generation of rainy events. Rainfall depth was generated with a normal asymmetric function (Sharpley and Williams, 1990).

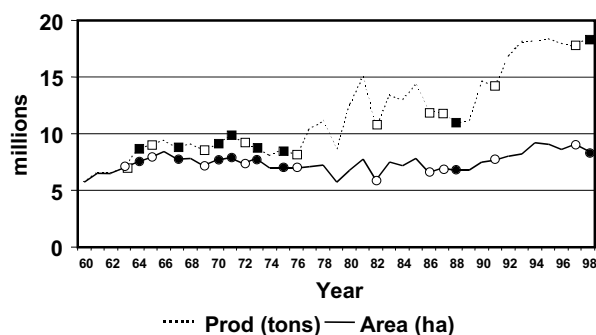


Fig. 1. Land-use with maize in Mexico and national production of maize. White squares and circles represent El Niño years, Black squares and circles represent El Viejo years.

EPIC calculated daily potential plant growth as a function of a crop-specific radiation-use efficiency and canopy-intercepted photosynthetic active radiation. Vapor-pressure deficit and CO₂ influenced the conversion of solar energy into plant biomass (Stockle *et al.*, 1992). Average daily air temperature determined the rate of photosynthesis, respiration, transpiration and the phenology of plant development. The level of nitrogen and phosphorus available in the soil also influenced the rate of plant growth. The crop yield is thus a result of the accumulated plant biomass multiplied by a harvest efficiency index that utilizes a non linear function of accumulated heat units, from zero in the moment of seeding up to the highest production value at crop maturity (Sharpley and Williams, 1990).

The hydrologic variables that occur in the cultivated lands, such as infiltration, overland runoff, percolation and movement of surface water, were estimated using the Numerical Curve Method, while water erosion was determined with the Modified Universal Soil Loss Equation (Williams, 1995).

Potential evapotranspiration (PET) and actual evapotranspiration (AET) were other variables of interest in the study because the changes in the patterns of precipitation and temperature affect water usage by the crop. PET was calculated using the Priestley-Taylor method (Priestly and Taylor, 1972) since there is a lack of daily data on solar radiation and wind velocity, while AET was computed using a procedure developed by Ritchie (1972), where plant transpiration is a function of PET and the leaf-area index of the crop. Direct evaporation of water from the soil was determined by the soil water content, the canopy cover that determines the amount of direct solar radiation reaching the soil and the wind velocity (Sharpley and Williams, 1990).

CHANGES IN CROP YIELD

Soils data, crop management practices information, and historical records of crop yield from 60 farms distributed throughout the country were utilized to construct the input data files of the EPIC model and to calibrate it. It was necessary to identify plausible simulations of crop yield for rain-fed maize, beans and wheat for each ENSO scenario.

Every farm in the study was assumed to be representative of thousands of farm units within an agricultural region of economic importance for national agriculture. Crop productivity in the region is a function of soils, date of seeding, farming practices, the applied inputs by farmers and climate conditions. For each farm, 30 years of crop production were simulated, applying each ENSO-climate scenario (EN, ENE, EV and N). This made possible an approximation of the statistic distribution of yield anomalies due to

ENSO-related climate variations. The approximation was necessary because statistics from distributions of observed crop yield anomalies held a considerable degree of uncertainty since at present the number of ENSO events in each category does not represent a reliable statistical sample. Only 6 EN, 2 SEN and 7 EV events had been observed from 1960 to 1989.

RESULTS AND DISCUSSION

The identification of changes in the precipitation and temperature patterns resulting from different ENSO phases was an important part of this study. Variations in precipitation and air temperature among different regions throughout the year are factors influencing crop development under rain-fed conditions. Table 1 shows the mean air temperature anomalies in four agricultural regions of the country. It indicates that the Arid and Semiarid region has higher temperatures in all seasons of the year during EN, SEN and EV episodes than during Neutral (N) years. The Temperate region of central Mexico experiences reductions in air temperature during spring and summer in EN and SEN years, while the Humid Tropical region tends to be cooler in the EN and EV years than in N years.

Table 1

Seasonal mean air temperature (°C) in Neutral years and deviation in El Niño (den), Strong El Niño (dsen), El Viejo (dev) years in different agroecological regions of Mexico

	ENSO Phase	Arid and Semiarid	Temperate	Dry Tropic	Humid Tropic
Dec-Jan-Feb	N	14.8	16.3	21.1	22.1
	den	0.6	0.0	0.4	0.7
	dsen	0.4	0.1	0.5	-0.1
	dev	0.1	0.3	0.2	-0.1
Mar-Apr-May	N	21.3	21.1	25.8	26.7
	den	0.6	-0.2	0.4	0.4
	dsen	0.4	-0.5	0.3	-0.6
	dev	0.3	0.2	0.4	0.2
Jun-Jul-Aug	N	26.9	20.8	26.9	26.8
	den	0.1	-0.6	0.3	0.0
	dsen	0.5	-0.5	-0.3	-0.4
	dev	0.8	0.1	0.6	0.2
Sep-Oct-Nov	N	21.8	18.9	24.9	25.0
	den	0.4	0.1	0.1	0.0
	dsen	-0.2	-0.1	-0.4	-0.8
	dev	0.3	-0.3	0.2	-0.1

ENSO caused significant rainfall variations among regions. The Arid and Semiarid region of northern Mexico is predisposed to rainfall increments for most part of the year during EN, SEN and EV episodes; however, a significant rainfall reduction occurs in the winter months during EV years (Table 2). The Temperate region suffers a decrease in rain during the EN and SEN winters, SEN springs and EV winters but experiences an increase in rainfall in EV summers. The Humid Tropical region is drier during summer and spring in EN and EV than in N years.

The analyses of the generated information indicated that EN and SEN winters tend to be humid in the north of the country, and EN and SEN summers are drier than those of N years. In the case of EV winters, drought conditions usually prevail all over the country, a situation that intensifies spring droughts. During EV summers, there is a significant increase in the amount of rainfall in central Mexico, but only a moderate increment in rain at the north.

The effects of anomalies in temperature and precipitation are reflected in the crop yield, particularly in the case of rain-fed crops. The application of the EPIC model made it

possible to approximate crop development under soil moisture stress caused by departures of rainfall from the normal pluvial pattern in each region (Figure 2). Figure 3 illustrates the changes in maize yield attributed to EN and EV anomalies. It shows that maize production in some Mexican states is highly sensitive to specific ENSO scenarios, with positive and negative effects. This is crucial for the national food security because the states in Figure 3 contribute more than 50% to the national maize production.

Rain-fed bean, most of which is produced in northern and southeastern Mexico, tends to manifest considerable interannual yield variations as a result of climate anomalies (Figure 4). Guerrero, Durango and Zacatecas show the greatest changes in bean production; this is significant considering that these states have allocated over a million hectares of land for bean cultivation. The six states alone in Figure 4 contribute more than 60% to the national bean production. It is important to highlight that in Chiapas, bean is a traditional alternative crop to mitigate the effects of droughty years, like El Niño years, in which maize cultivation results in low yields. Droughty years in southern Mexico are highly related to EN and SEN summers.

Table 2

Seasonal precipitation (mm) in Neutral years and percent of deviation in El Niño (den), Strong El Niño (dsen), El Viejo (dev) years in different agroecological regions of Mexico.

	ENSO Phase	Arid and Semiarid	Temperate	Dry Tropic	Humid Tropic
Dec-Jan-Feb	N	53.8	35.6	54.4	141.2
	den	3.7	-26.5	29.3	-10.3
	dsen	74.4	-0.1	54.8	43.4
	dev	-48.7	-39.4	0.2	36.8
Mar-Apr-May	N	57.3	81.7	84.2	134.1
	den	10.3	5.0	161.3	-11.9
	dsen	255.9	-25.2	653.3	-48.9
	dev	69.4	47.9	493.5	-1.9
Jun-Jul-Aug	N	229	420	421.6	725.3
	den	16.3	1.4	18.0	-2.9
	dsen	42.9	21.3	26.4	13.7
	dev	8.1	4.0	-5.6	0.9
Sep-Oct-Nov	N	151.8	172.8	250.3	532.7
	den	2.8	15.7	14.5	-8.9
	dsen	41.4	22.4	9.8	-25.9
	dev	1.7	12.5	0.3	-10.0

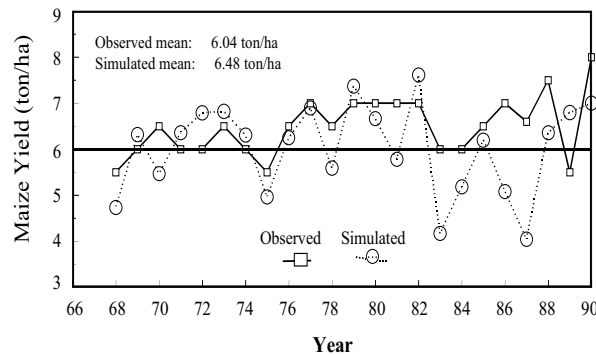


Fig. 2. Model validation using historical records of climate and maize yield from Ameca, Jalisco, Mexico.

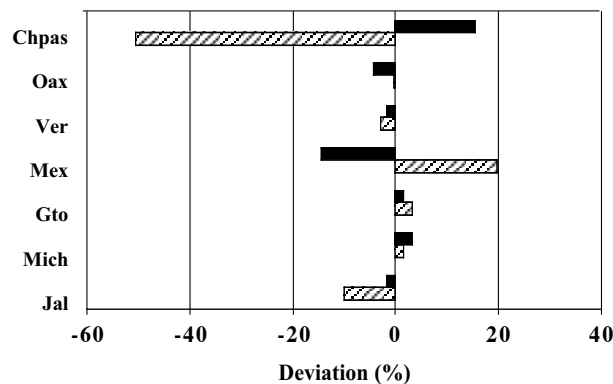


Fig. 3. Maize yield deviations of representative farms located in important states for national maize production. Black strips represent El Niño years and gray strips represent El Viejo years.

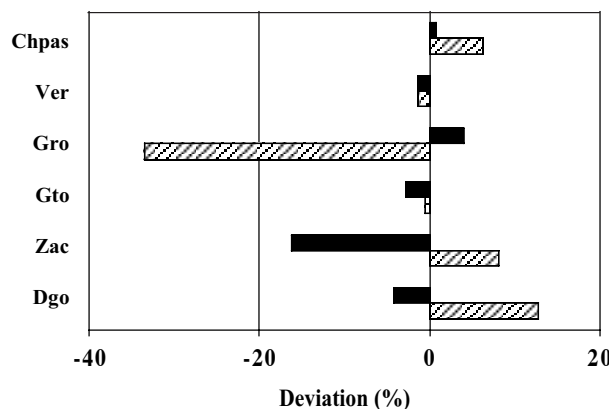


Fig. 4. Bean yield deviations of representative farms located in important states for national bean production. Black strips represent El Niño years and gray strips represent El Viejo years.

In addition, the model enabled the assessment of soil moisture deficits and excesses triggered by El Niño climatic anomalies in Mexico. For every day of water stress (determined by the deficit or excess of soil water) maize lost 97kg/ha, beans 38kg/ha, and wheat 69kg/ha, a worrisome situation considering that an average El Niño brings about around 15.3, 10.1 and 11.5 days of water stress for the aforementioned crops, respectively.

The impact of ENSO on natural resources in each agricultural region depends on the ENSO variant manifested - El Niño or El Viejo - and its intensity. This was estimated by the amount of soil erosion in the cultivated field during the EN years. In the case of the Humid Tropical region, none of the ENSO scenarios modifies the regular erosion pattern; however, in the Semiarid region, a considerable amount of soil losses during El Niño years was detected. During EN and SEN years, northern Mexico is enormously affected by storms of high intensity, short duration and limited extent. Usually, precipitation in EN years is less than in EV and N years, but the increase in soil erosion is provoked by the few storms that release a large part of the total annual volume of water from precipitation. In general, it has been identified that there exists a climatic pattern that induces an increment in erosion, depending on the dryness of the agricultural region. This has given rise to the assumption that El Niño directly affects those regions with advanced stages of desertification.

Finally, the ENSO-related changes in precipitation and temperature that affect crop yields have forced state and federal governments to implement mitigation actions for droughts, in order to reduce the impact of the climate phenomena on the farmer's economy and the national economy as a whole. This study made it possible to inform SAGAR, the Mexican Ministry of Agriculture, of the expected changes in crop production and hence, to implement an agricultural conversion plan for all country states. The land-use conversion plans under ENSO included changes in species and varieties as well as changes in the planting dates and financial support to farmers, in order that national agricultural productivity may be ensured for the 100 million inhabitants of Mexico.

CONCLUSIONS

Based on the results of this research on the ENSO climate phenomena, aimed to identify their impact on agricultural production of basic crops using a process-based biophysical simulation model, it is evident that ENSO-derived climate scenarios induce crop yield changes with impacts on regional and national agricultural productivity.

Alterations in precipitation and temperature patterns vary among regions, depending on the ENSO phase and its

intensity. On a national scale, the study identified drier winters under the influence of El Viejo, more humid winters during El Niño years, dry summers in El Niño years and moist summers in El Viejo years. Such patterns of precipitation due to ENSO phenomena are the outcomes of this research that are relevant for decision-making on crop management in Mexico.

Regarding changes in crop yields related to ENSO, EV adversely affects rain-fed bean production in the northern states, in the same way that maize production in the south-east is affected by EN and SEN years. The Central Temperate states are affected in varying ways during the different phases of ENSO. For example, maize production in the state of Mexico suffers the detrimental effects of El Niño but benefits from El Viejo presence due to an increase in rainfall.

Finally, it is important to mention the increase in soil erosion during El Niño years. During EN and SEN, a reduction in precipitation is commonly observed, but such rainfall reduction is linked to high-intensity short-duration storms that create a great amount of runoff. The reduction in winter rains during EV years holds major implications for livestock production in the north of Mexico, since it adversely affects the growth of grass in spring, thereby reducing forage production needed for the extensive grazing systems.

APPENDIX

THE EPIC MODEL

The Erosion-Productivity Impact Calculator (EPIC) (Williams *et al.*, 1984) model was developed to assess the effect of soil erosion on soil productivity and crop yield estimation in areas up to 100 ha of size having homogeneous weather, soils and management systems. The purpose of this section is to describe the governing equations of major simulated processes by the model, only.

Surface Runoff. The runoff component of the EPIC model simulates overland flow in terms of runoff volume and peak rate, given daily rainfall amounts. Surface runoff is predicted for daily rainfall using the curve number equation

$$Q = \frac{(R - 0.2s)^2}{R + 0.8s}, \quad R > 0.2s \quad (1)$$

$$Q = 0.0 \quad R \leq 0.0,$$

where Q is the daily runoff, R is the total daily rainfall, and s is a retention parameter that depends of soils, land use, management and slope. The parameter s is related to the equation

$$s = 254 \left(\frac{100}{CN} - 1 \right) \quad (2)$$

the constant, 254 in Eq. (2) give s in mm.

Peak Runoff Rate. EPIC estimates peak runoff rate based on the modified Rational Formula

$$q_p = (\rho)(r)(A)/360, \quad (3)$$

where q_p is the peak runoff rate in m^3/s , ρ is a runoff coefficient expressing the watershed infiltration characteristics, r is the rainfall intensity in mm/hr for the watershed's time of concentration, and A is the drainage area in ha. The runoff coefficient can be calculated for each storm if the amount of rainfall and runoff are known:

$$\rho = \frac{Q}{R}. \quad (4)$$

Since R is input and Q is computed with Eq. (1), ρ can be calculated directly. Rainfall intensity can be calculated with the relationship

$$r = \frac{R_{tc}}{t_c}, \quad (5)$$

where R_{tc} is the amount of rainfall in mm during the watershed's concentration time, t_c in h. The value of R_{tc} can be estimated by developing a relationship with total R .

Percolation. The EPIC percolation component uses a storage routine technique to simulate flow through soil layers. Flow from a soil layer occurs when soil water content exceeds field capacity. Water drains from the layer until the storage returns to field capacity. The reduction in soil water content is simulated with the equation

$$SW_l = (SW_{ol} - FC_l) \exp(-\Delta t / TT_l) + FC_l, \quad (6)$$

where SW and SW_o are the soil water contents at the end and the start of the time interval Δt (24 h) and the TT is the travel time through the layer l in h. Thus, daily percolation can be computed by taking the difference between SW and SW_o :

$$O_l = (SW_{ol} - FC_l)[1.0 - \exp(-\Delta t / TT_l)], \quad (7)$$

where O is the percolation rate for the layer l in mm/d. Travel time through a layer is computed with the liner storage equation

$$TT_l = \frac{PO_l - FC_l}{SC_l}, \quad (8)$$

where PO is the porosity in mm, FC is field capacity in mm, and SC is saturated hydraulic conductivity in mm/h.

Evaporation. The model offers estimating potential evaporation using one of four methods: Hargreaves and Simani (1985), Penman (1948), Priestley-Taylor (Priestley-Taylor, 1972) and Penman-Monteith (Monteith, 1965). In this study the Penman-Monteith equation was used:

$$E_o = \left(\frac{\delta}{\delta + \gamma} \right) \left(\frac{h_o - G}{HV} \right) + \left(\frac{\gamma}{\delta + \gamma} \right) f(V)(e_a - e_d), \quad (9)$$

where E_o is the potential evaporation in mm, δ is the slope of the saturation vapor pressure curve in kPa/°C, γ is a psychrometer constant in kPa/°C, h_o is the net radiation in MJ/m², G is the soil heat flux in MJ/m², HV is the latent heat of vaporization in MJ/kg, $f(V)$ is a wind speed function in mm/d/kPa, e_a is the saturation vapor pressure at mean air temperature in kPa, and e_d is the vapor pressure at mean air temperature in kPa.

Weather. The weather variables necessary for driving EPIC are precipitation, air temperature and solar radiation. If the Penman methods are used to estimate potential evaporation, wind speed and relative humidity are also required.

Precipitation. The EPIC precipitation model developed by Nicks (1974) is a first-order Markov chain model. Thus, input for the model must include monthly probabilities of receiving precipitation. On any given day, the input must include information as to whether the previous day was dry or wet. A random number (0-1) is generated and compared with the appropriate wet-dry probability. If the random number is less than or equal to the wet dry probability, precipitation occurs on that day. Random numbers greater than the wet-dry probability give no precipitation. If the wet-dry probabilities are not given, the average monthly numbers of rainy days may be substituted. The probability of a wet day is calculated from the number of wet days:

$$PW = NWD / ND, \quad (10)$$

where PW is the probability of a wet day, NWD is the number of rainy days, and ND is the number of days. The probability of a wet day after a dry day can be estimated as the fraction of PW :

$$P(W/D) = \beta PW, \quad (11)$$

where $P(W/D)$ is the probability of a wet day following a dry day and where β is a fraction usually in the range of 0.6 to 0.9. The probability of a wet day following a wet dry can be calculated directly by using the equation:

$$P(W/W) = 1.0 - \beta + P(W/D), \quad (12)$$

where $P(W/W)$ is the probability of a wet day after a wet day.

When precipitation event occurs, the amount is generated from a skewed normal daily precipitation distribution that uses the mean and standard deviation of daily observed rainfall.

Air Temperature and Solar Radiation. EPIC generates temperature and solar radiation, which are mutually correlated with rainfall. The residuals of daily maximum and minimum air temperature and solar radiation are generated from a multivariate normal distribution. It implies that temperature and solar radiation variables are normally distributed and that the serial correlation of each variables can be described by a first-order linear autoregressive model. Thus, the model requires monthly means and standard deviations.

Crop Growth. Annual crops are simulated from planting date to harvest date or until the accumulated heat units equal the potential heat units for the crop. Perennial crops maintain their roots systems throughout the year, although they may become dormant after frost. They start growing when average daily air temperature exceeds the base temperature. Phenological development of the crop is based on daily heat unit accumulation. It is computed by using the equation

$$HU_k = \left(\frac{T_{mx,k} + T_{mn,k}}{2} \right) - T_{b,j}, \quad HU_k \geq 0, \quad (13)$$

where HU , T_{mx} , and T_{mn} are the values of heat units, maximum temperature, and minimum temperature in °C on day k , and T_b is the crop-specific base temperature in °C (no growth occurs at or below T_b) of crop j . A heat unit index (HUI) ranging from 0 at planting to 1 at physiological maturity is computed as follows:

$$HUI_i = \frac{\sum_{k=1}^i HU_k}{PHU_j}, \quad (14)$$

where HUI is the heat unit index for day i and PHU is the potential heat units required for the maturation of crop j . The value of PHU may be inputted or calculated by the model from normal planting and harvest dates. Potential growth is computed from intercepted solar radiation, estimated by the Beer's law equation

$$PAR_i = 0.5 (RA)_i [1 - \exp(-0.65 LAI_i)], \quad (15)$$

where PAR is intercepted photosynthetic active radiation in MJ/m^2 , RA is solar radiation in MJ/m^2 , LAI is the leaf area index, and subscript i is the day of the year.

Soil and Plant Evaporation. The model computes evaporation from soils and plants as the effects of solar radiation and wind effects as

$$E_p = \left(\frac{(E_o)(LAI)}{3.0} \right), \quad 0 \leq LAI \leq 3.0 \quad (16)$$

$$E_p = E_o \quad LAI > 3.0, \quad (17)$$

where E_p is the predicted plant water evaporation rate in mm/d. Potential soil water evaporation is simulated by considering soil cover according the following equation:

$$E_s = (E_o)(EA), \quad (18)$$

where E_s is the potential soil water evaporation rate in mm/d.

Water Use. Water potential use from soil surface to any root depth is estimated with the function

$$U_{pi} = \left(\frac{E_{pi}}{1 - \exp(-\Lambda)} \right) \left(1 - \exp \left[-\Lambda \left(\frac{Z}{RZ} \right) \right] \right), \quad (19)$$

where U_p is the total water use in rate in mm/d to depth Z in m on day i , E_p is estimated with equations 16 and 17, RZ is the root zone depth in m, and Λ is a water distribution parameter.

BIBLIOGRAPHY

- CANBY, T. Y., 1984. El Niño's ill wind. *National Geographic*, Feb. 144-183.
- CANE, M. A., G. ESHEL and R. W. BUCKLAND, 1994. Forecasting Zimbabwean maize yield using eastern equatorial Pacific sea surface temperature. *Nature*, 370, 204-205.
- GLANTZ, M. H., 1986. Currents of Change: El Niño's impact on climate and society. Cambridge University Press, pp.194.
- IZAURRALDE, R. C., N. J. ROSENBERG, R. A. BROWN, D. M. LEGLER, M. TISCAREÑO LÓPEZ and R. SHRINIVASAN, 1998. Modeled effects of moderated and strong "Los Niños" on crop productivity in North America. *J. Agricultural and Forest Meteorology*, 94, 259-268.
- NICKS, A. D., 1974. Stochastic generation of the occurrence, pattern, and location of maximum amount of daily rainfall. Pp. 154-171, *In: Proc. Symp. Statistical Hydrology*, Aug.-Sept. 1971. Tucson, AZ. U.S. Dept. of Agriculture. Misc. Publ. No. 1275.
- PRIESTLEY, C. H. B. and R. J. TAYLOR, 1972. On the assessment of surface heat flux and evaporation using large-scale parameters. *Mon. Weather Rev.*, 100, 81-92.
- RASMUSSEN, E. M., 1985. El Niño and variations in climate. *American Scientist*, 73, 168-173.
- RICHARDSON, C. W., 1981. Stochastic simulation of daily precipitation, temperature, and solar radiation. *Trans. ASAE*, 25(3), 735-739.
- RITCHIE, J. T., 1972. A model for predicting evaporation from a row crop with incomplete cover. *Wat. Res. Res.*, 8, 1204-1213.
- SHARPLEY, A. N. and J. R. WILLIAMS, 1990. The nutrient component of EPIC. Chapter 7, pp. 152-166. *In: A.N. Sharpley and J.R. Williams (eds.) EPIC – Erosion/Productivity Impact Calculator: 1. Model Documentation*. U.S. Dept. Agric. Tech. Bull., No. 1768.
- SOLOW, A. R., R. F. ADAMS, K. J. BRYANT, D. M. LEGLER, J. J. O'BRIEN, B. A. MCCARL, W. NAYDA and R. WEIHER, 1997. The value of improved ENSO prediction to U.S. agriculture. *Climate Change* (submitted).
- STOCKLE, C. O., P. T. DYKE, J. R. WILLIAMS, C. A. JONES and N. J. ROSENBERG, 1992. A method for estimating direct and climatic effects of rising atmospheric carbon dioxide on growth and yield of crops: Part II – Sensitivity analysis at the three sites in the Midwestern USA. *Agricultural Systems*, 38, 239-256.
- TRENBERTH, K. E. and G. W. BRANDSTADTER, 1992. Issues in establishing causes of the 1988 drought over North America. *J. Clim.*, 5, 159-172.
- WILLIAMS, J. R., 1995. The EPIC model. *In: V.P. Singh (editor), Computer models of watershed hydrology*, Water, Resources Research. Public. Highlands Ranch, CO. pp.909-1000.

WILLIAMS, JR., C. A. JONES and P. T. DYKE, 1984. The EPIC model and its applications. pp. 111-121 In Proc. ICRISAT-IBSNAT-SYSS Symp. on Minimum Data Sets for Agrotechnology Transfer, March 1983, Hyderabad, India.

Mario Tiscareño López¹, Alma Delia Báez González², César Izaurralde³, Norman J. Rosenberg⁴ and Jaime Salinas García⁵

¹ *Instituto Nacional de Investigaciones Forestales Agrícolas y Pecuarias, Campo Experimental Pabellón, Km 32 Carr. Ags-Zac, AP 20, 20660 Pabellón de Arteaga, Aguascalientes, México, Tel (495) 8-01-67*

Email: mtiscareno@infosel.net.mx

² *Instituto Nacional de Investigaciones Forestales Agrícolas y Pecuarias, Campo Experimental Pabellón, Km 32 Carr. Ags-Zac, AP 20, 20660 Pabellón de Arteaga, Aguascalientes, México, Tel (495) 8-01-67,*

Email: baez_07@yahoo.com.mx

³ *Battelle, Pacific National Northwest Laboratory, 901 D Street, SW, Suite 900, Washington, D.C 20024-2115, Tel. (202) 646-5029,*

Email: cesar.Izaurralde@pnl.gov

⁴ *Battelle, Pacific National Northwest Laboratory, 901 D Street, SW, Suite 900, Washington, D.C 20024-2115, Tel. (202) 646-5029,*

Email: nj_rosenberg@pnl.gov

⁵ *Instituto Nacional de Investigaciones Forestales Agrícolas y Pecuarias, Campo Experimental de Rio Bravo, Km 61 Carr. Matamoros-Reynosa, Mpio. De Rio Bravo, Tamaulipas, México, Tel (495) 8-01-67,*

Email: jrs050@yahoo.com